

Red phosphorus and gold nanoparticles as novel candidates for intact cell MALDI TOF MS.

Estudiant: Cristina Font Calvarons

Grau en Biotecnologia

Correu electrònic: u1921609@campus.udg.edu

Tutora: Victòria Salvadó

Cotutor: Petr Vanhara

Empresa / institució: Masaryk university

Vistiplau tutor (i cotutor):

Nom de la tutora: Victòria Salvadó

Nom del cotutor: Petr Vanhara

Empresa / institució: Masaryk university

Correus electrònics:

pvanhara@med.muni.cz

victoria.salvado@udg.edu

Data de dipòsit de la memòria a secretaria de coordinació:

ACKNOWLEDGMENTS

I wish to thank various people for the contribution to this project.

From the department of Histology and Embryology, Faculty of Medicine, Masaryk University, I would like to express my deep gratitude to my supervisor Dr. Petr Vaňhara, Ph.D., for guidance and encouragement throughout the project. I would like to offer my special thanks as well to Mgr. Kateřina Kratochvílová for her advice and help with the cultivation of cells. Many thanks as well to Mgr. Lukáš Kučera, Ph.D. for helping me with the preparation of samples for mass spectrometry.

From the department of Chemistry, Faculty of Science, Masaryk University, I would like to express my very thanks to Professor Josef Havel and Mgr. Lenka Kolářová for helping me with the mass spectrometry analyses and resolving my doubts about this technique.

Finally, last but not least, I would like to extend my thanks to Dra. Victòria Salvadó from Universitat de Girona and to Professor MVDr. Aleš Hampl, CSc. from the department of Histology and Embryology, Faculty of Medicine, Masaryk University for making all the arrangements and enabling me the opportunity to finish my bachelor studies in Masaryk University, under the ERASMUS program.

LIST OF ABBREVIATIONS

a.u	Arbitrary units
AuNFs	Flower-like gold nanoparticles
AuNPs	Gold nanoparticles
CB	Citrate buffer
DMEM	Dulbecco's modified eagle medium
FBS	Fetal bovine serum
HEK 293	Human embryonic kidney cell line
MALDI	Matrix-assisted laser desorption/ionization
LDI	Laser desorption/ionization
MTT	3-(4,5-dimethylthiazol-2-yl)-2,5-diphenyltetrazolium bromide
MS	Mass spectrometry
<i>m/z</i>	Mass to charge
PBS	Phosphate buffered saline
PVP	Poly-(N-vinyl-2-pyrrolidone)
Red AuNPs	Red gold nanoparticles (polyhedral gold nanoparticles)
Red P	Red phosphorus
SA	Sinapinic acid
SALDI	Surface-assisted laser desorption/ionization
TOF	Time-of-flight

SUMMARY

Mass spectrometry (MS) is a widely used technique in many different fields such as proteomics, drug discovery and genomics. It measures the m/z ratio of the different components of a sample producing a mass spectrum, which has to be calibrated with internal or external calibration standards. In this project we studied if flower-like gold nanoparticles (AuNFs), red gold nanoparticles (red AuNPs) and red phosphorus (red P) could be used as internal calibration standards for matrix assisted laser desorption/ionization (MALDI) time-of-flight (TOF) MS analyses of intact eukaryotic (HEK 293) cells.

These elements form distinct monoisotopic clusters by laser desorption/ionization (LDI) which makes them ideal for being used as external calibration standards. When studying their capability as internal calibration standards for MALDI TOF MS technique we realized that sinapinic acid (SA) interacted with gold nanoparticles (AuNPs) impeding gold clusters to appear on the spectrum. Still AuNPs could not be used as internal calibration standards when we removed the matrix using surface-assisted laser desorption/ionization (SALDI) TOF MS technique as no organic compounds of HEK 293 cells at a high m/z range could be seen on the spectrum. Thus, we let crystallize the matrix with the cells before adding the AuNFs. By doing so, we minimized the interaction between sinapinic acid and gold and at the same time enhanced the ionization of high molecular compounds of HEK 293 cells. We partially succeeded by following this methodology as HEK 293 organic compounds could be seen at a high m/z range but gold clusters could only be seen at a low m/z range (800 m/z). The same methodology was used for red P and obtained better results. Phosphorus clusters could be seen up to 2600 m/z together with HEK 293 organic compounds at a high m/z range.

Cytotoxicity of these three elements was also studied in HEK 293 cells. Gold nanoparticles have numerous applications in the medicine field, thus studying its toxicity is of great importance. Red phosphorus is not as widely used but still its toxicity was also studied. Cell viability and proliferation was not affected by AuNPs whereas it was negatively altered by red phosphorus in dose dependent manner.

A further analysis was done by comparing the mass spectra of treated cells (with AuNPs and red P) and non-treated cells. We determined that AuNPs geometry is an important issue to be considered. Regarding red P, no differences were observed when comparing the mass spectra.

RESUMEN

La espectrometría de masas (EM), es una técnica muy utilizada en ámbitos diversos tales como la proteómica, genómica y en el descubrimiento de nuevos fármacos. En EM, se mide la relación m/z de los iones generados por la muestra al ionizarse en fase gaseosa obteniendo un espectro de masas que se tiene que calibrar con patrones internos o externos. En este proyecto, se ha evaluado la aplicación de las nanopartículas de oro con forma de flor (AuNFs), nanopartículas de oro rojas (red AuNPs) y el fósforo rojo (P rojo) como posibles patrones de calibración internos de células eucariotas (HEK 293) en MALDI TOF MS (matrix assisted laser desorption/ionization time-of-flight).

El oro y el fósforo, al ser elementos monoisotópicos, forman picos diferenciados en el espectro de masas al ser ionizados por medio del LDI (laser desorption/ionization). Esta característica es muy importante para su aplicación como patrones de calibración externos. Durante el estudio con la técnica MALDI TOF MS, se observó que el ácido sinapínico (SA) impide la aparición de los picos de oro en el espectro de masas debido a que esta matriz interactúa con las nanopartículas de oro (AuNPs).

Se optó por eliminar la matriz y utilizar la técnica SALDI (surface-assisted laser desorption/ionization) como fuente de ionización, pero no se consiguió ionizar los compuestos orgánicos de elevado peso molecular de HEK 293. Finalmente, cristalizando las células con la matriz previa a la adición de las AuNFs, se consiguió disminuir la interacción entre el ácido sinapínico y las AuNFs y, además, se obtuvo la ionización de los compuestos orgánicos de HEK 293 de elevado peso molecular. Aun así, con este método solo se observaron picos de oro hasta 800 m/z . Cuando se substituyeron las AuNFs por el P rojo y utilizando la misma metodología se obtuvieron en el espectro de masas picos de fósforo en un rango m/z más elevado (2600 m/z) junto con compuestos orgánicos de elevado peso molecular de las células.

También se estudió la citotoxicidad de AuNPs y P rojo en el HEK 293. En cuanto a la viabilidad y proliferación de las células, no se observaron diferencias al ser tratadas con AuNPs. En cambio, al ser tratadas con P rojo, ambos parámetros se vieron afectados en función de la dosis utilizada.

Asimismo, se compararon los espectros de masas de células tratadas (con AuNPs y P rojo) y células no tratadas. No se observaron diferencias en células tratadas con P rojo, mientras que se observó que la geometría de las AuNPs afecta de forma distinta a las células.

RESUM

L'espectrometria de masses (EM), és una tècnica àmpliament utilitzada en diversos àmbits com la proteòmica, genòmica i descobriment de nous fàrmacs. La EM mesura la relació m/z dels ions generats al ionitzar la mostra en fase gasosa obtenint-se un espectre de masses que s'ha de calibrar amb patrons interns o externs. En aquest projecte, s'ha avaluat l'ús de les nanopartícules d'or amb forma de flor (AuNFs), nanopartícules d'or vermelles (red AuNPs) i el fòsfor vermell (P vermell) com a patrons de calibració interns per l'anàlisi mitjançant MALDI TOF MS (matrix assisted laser desorption/ionization time-of-flight) de cèl·lules eucariotes (HEK 293).

L'or i el fòsfor, al ser monoisotòpics formen pics diferenciats en l'espectre de masses quan són ionitzats mitjançant LDI (laser desorption/ionization). Això els fa ideals per a ser utilitzats com a patrons externs de calibració. En l'estudi de la seva utilització com a patrons de calibració interns pel MALDI TOF MS, es va observar que l'àcid sinapínic (SA) interactua amb les nanopartícules d'or (AuNPs) impedit l'aparició de pics d'or a l'espectre. Traient la matriu i utilitzant SALDI (surface-assisted laser desorption/ionization) com a font de ionització no es solucionava el problema ja que els compostos orgànics d'elevada massa molecular de HEK 293 no s'ionitzaven i no apareixien a l'espectre. Finalment, afegint AuNFs, després de la cristal·lització de la matriu i les cèl·lules, no només es disminuïa la interacció entre l'àcid sinapínic i les AuNFs sinó que també s'aconseguia ionitzar els compostos d'elevat pes molecular de les HEK 293. Tot i això, amb aquest mètode només s'observaven pics d'or fins a 800 m/z a l'espectre de masses. Pel que fa al P vermell, i seguint la mateixa metodologia, s'obtenien pics de P en un interval m/z més elevat (2600 m/z) juntament amb els pics corresponents als compostos orgànics d'elevat pes molecular de les cèl·lules.

També es va estudiar la citotoxicitat de les AuNPs i el P vermell en les HEK 293. Si bé la viabilitat i proliferació de les cèl·lules no es van veure afectades per les AuNPs, sí que es van veure afectades en funció de la dosis, pel P vermell.

També es van comparar els espectres de masses entre cèl·lules tractades (amb AuNPs i P vermell) i cèl·lules no tractades. No es van observar diferències en les cèl·lules tractades amb P vermell, mentre que es va observar que la geometria de les AuNPs afecta a les cèl·lules de diferent manera.

INDEX

1. INTRODUCTION	6
1.1 Matrix-assisted laser desorption/ionization (MALDI)	7
1.2 Laser desorption/ionization (LDI).....	8
1.3 Surface-assisted laser desorption/ionization (SALDI)	8
1.4 Time-of-flight (TOF)	9
1.5 Calibration of the mass spectra	9
1.5.1 Gold nanoparticles (AuNPs)	10
1.5.1.1 Flower-like gold nanoparticles (AuNFs)	10
1.5.1.2 Red gold nanoparticles (red AuNPs) or polyhedral gold nanoparticles	11
1.5.2 Red phosphorus	11
1.6 HEK 293 cells.....	12
2. OBJECTIVES	12
3. METHODOLOGY	13
3.1 LDI/MALDI/SALDI TOF MS.....	13
3.1.1 Treatments.....	13
3.1.2 Sample preparation.....	14
3.1.3 Reagents.....	14
3.1.3.1 Synthesis of flower-like gold nanoparticles (AuNFs).....	14
3.1.3.2 Synthesis of red gold nanoparticles (Red AuNPs)	15
3.1.3.3 Synthesis of red phosphorus (Red P)	15
3.1.3.4 Sinapinic acid (SA).....	15
3.1.3.5 Amonium bicarbonate (ABC)	15
3.1.3.6 Citrate buffer (CB).....	15
3.2 MTT assay	15
3.2.1 Cultivation of cells for the MTT assay.....	15
3.2.2 Reagents.....	16
3.2.2.1 MTT reagent	16
3.2.2.2 Detergent	16
3.3 Growth curve	16
3.3.1 Cultivation of cells for the growth curve	16
4. RESULTS	17
5. DISCUSSION.....	25
6. CONCLUSIONS.....	29
7. REFERENCES.....	29

1. Introduction

Mass spectrometry is a widely used technique which has been applied in many different fields such as proteomics, drug discovery, clinical testing, genomics, environment, geology, etc. It measures the mass to charge ratio (m/z) of gaseous ions from the sample being studied to identify and quantify molecules in simple and complex mixtures.^[1, 2]

The components of a mass spectrometer can be divided into:

- Sample inlet to introduce the sample that will be analyzed.
- Ion source which will produce gaseous ions from the sample of interest.
- Mass analyzer which will separate the ions formed in the ion source.
- Detector which will detect the ions and record the relative abundance of each ion from the sample.
- Finally, a mass spectrum is obtained from the signals of the detector.

Mass spectrometers function under vacuum so that the air molecules don't interfere with the trajectory of the ion's produced from the sample and to avoid as well non-specific reactions -between the air molecules and the ions- which would increase the complexity of the spectrum.^[3]

There are many different components and instruments that can serve as a sample inlet, ion source, mass analyzer and detector (**Fig. 1**)

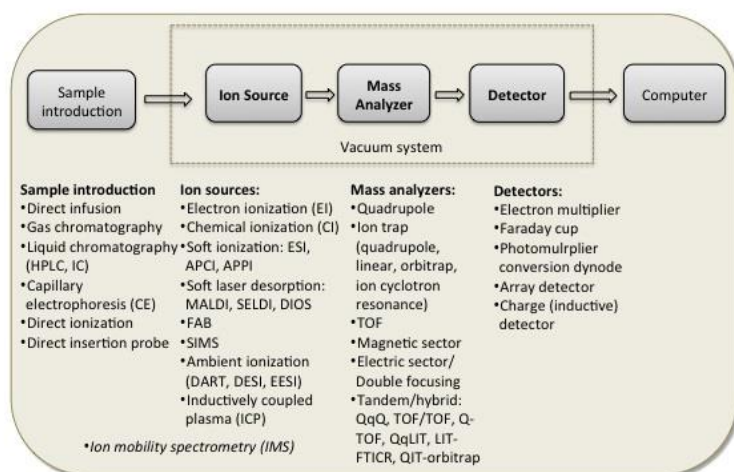


Figure 1. Components of mass spectrometry. Adapted from [4].

This project will study the use of different calibration standards of mass spectra in matrix-assisted laser desorption/ionization (MALDI) and surface-assisted laser desorption/ionization (SALDI) as the ion sources in the ionization of complex samples such as cells; thus the sample inlet will be a plate/target. The mass analyzer will be time-of-flight (TOF) for both ion sources.

1.1 Matrix-assisted laser desorption/ionization (MALDI)

Matrix assisted laser desorption/ionization MALDI is a soft ionization technique, which means that analytes are transferred intact into the gas phase. This makes the mass spectra easier to analyze, thus, it has become a very useful ionization technique in mass spectrometry.

The sample is co-crystallized with a large amount of matrix, which is usually a solution of low molecular weight organic compounds able to solubilize the sample without chemical reactivity and with strong absorption at the laser wavelength.^[5] There are different types of lasers that can be used, Nitrogen (337nm), Nd:YAG μ 3 (355nm), Nd:YAG μ 4 (266nm), Er:YAG (2.94 μ m) and CO₂ (10.06 μ m). Nitrogen UV laser 337nm is the most common one because it is economic and easy to manage.^[3]

The matrix minimizes sample damage from the laser beam by absorbing the incident laser energy which causes its sublimation together with the sample.^[6] The matrix then transfers protons to the different molecule components of the sample, thus ionizing them. **Figure 2** shows the ionization process of MALDI.

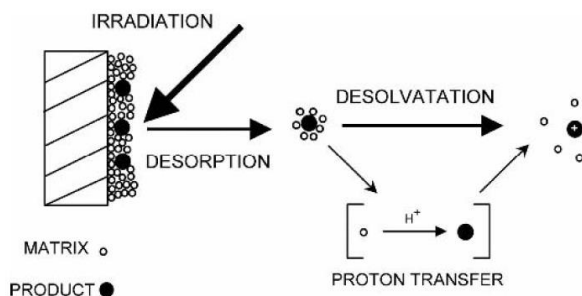


Figure 2. Ionization of the sample in MALDI. Adapted from [3].

MALDI has become one of the most used ionization source for biomolecules such as DNA, proteins, lipids, etc. since its discovery. The reason for it is its sensitivity, simplicity, tolerance to impurities such as salts and detergents and the production of mostly single charged ions which makes easier the analysis of the mass spectra.^[7, 8]

Despite all these benefits, MALDI has some problems:^[5, 9, 10]

- The analyte has to be soluble with the matrix and co-crystallize with it.
- The co-crystallization is not homogenous which leads to “hot (sweet) spots” which results in a fluctuating signal intensity and poor reproducibility.
- The matrix can interfere with low molecular compounds of the sample, so it is difficult to analyze low mass samples or samples with similar mass as the matrix.
- Difficulties in detecting poor ionized molecules.

To overcome these problems, laser desorption/ionization (LDI) and matrix-free surface-assisted laser desorption/ionization (SALDI) started to be developed as alternatives.^[11]

1.2 Laser desorption/ionization (LDI)

LDI involves the irradiation of the sample without the use of any matrix. Its applicability is limited because of the restricted mass range for analysis due to the fragmentation of the analyte.^[12]

This technique can effectively be used with samples that contain compounds with similar ionization properties as MALDI matrices. For example, it has recently been stated that LDI can be directly conducted in Lichen extracts without the use of any matrix due to the photo-absorbing properties observed for most groups of Lichens metabolites.^[13]

The use of assisting material for LDI such as small energy-absorbing molecules improves the mass spectra analysis, as they absorb the laser radiation and transfer it to the analytes minimizing thus their fragmentation.^[12] Surface enhanced laser desorption/ionization (SALDI) is an example for that.

1.3 Surface-assisted laser desorption/ionization (SALDI)

SALDI involves the use of an inorganic matrix, usually nanoparticles, that will absorb the laser energy and transfer it to the analytes of the sample, as shown in **Figure 3**.^[11,14]

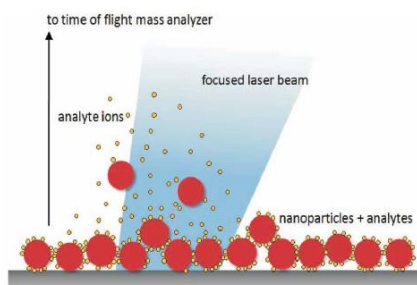


Figure 3. Ionization of the sample in SALDI. Adapted from [14].

Nanoparticles are microscopic particles between 1-100 nm size with uniform parameters and properties.^[15] As a result to their small size, the overall surface-to-volume ratio is increased, improving the interaction with the sample, and thus enhancing the ionization of the analytes.^[12]

The first approaches with SALDI were done by Tanaka *et al.* by using 30nm cobalt powders to detect proteins and polymers with molecular weights up to 25Kda.^[16] Much more approaches with different nanostructured substrates have been studied since then and are mainly classified into 3 groups:^[11]

- Metal-based, for example gold nanoparticles.
- Carbon based, for example diamonds.
- Semiconductor based, for example, nanopillars and nanocavity arrays.

Some current terms for the ionization process have arisen according to the nanomaterial used, but the most common terminology which involves all of them is SALDI.^[14]

AuNPs as a metal-based substrate will be used in this project.

1.4 Time-of-flight (TOF)

Time-of-flight (TOF) is a mass analyzer. Its function is to separate ions according to their mass to charge ratio by the speed they travel before reaching the detector.^[17] (Fig. 4)

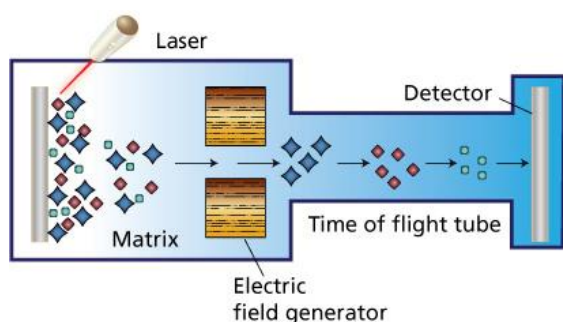


Figure 4. Matrix assisted laser desorption/ionization, time-of-flight analyzer. Adpated from [18].

As seen in **Figure 4**, once the sample is ionized, the ions are then accelerated with the same amount of energy with an electrostatic field through a metal flight tube subjected to vacuum until they reach the detector. The ions start at the same time as they were accelerated with the same amount of energy but they arrive at the detector on different times proportionally to their m/z . The lighter ones will arrive earlier than the heavier ones.^[19]

1.5 Calibration of the mass spectra

As mentioned above, once the ions are separated by TOF mass analyzer, they are directed towards the detector which will measure their intensity and display them into a mass spectra plot.

The mass to charge displayed in the plot should be calibrated using external or internal calibration standards with molecules of known masses. By doing so, the effects of substrate to substrate and spot to spot that can affect reproducibility are mitigated, and thus, an accurate spectra is obtained.^[11] In external calibration, the calibration standard is placed into one or more spots of the target and the parameters are then used for calibrating all other samples of interest. In the case of internal calibration, the calibration standard is mixed with the sample of interest so that each sample of interest will have its own calibration standard.^[20]

The external calibration is not as precise as the internal calibration as alterations in the strength of the electric field, instrumental drifts or changes in some environmental factors such as temperature or atmospheric pressure may occur between different spots on the same target.^[21, 22]

The internal calibration is not perfect though, because some calibration standards may be suppressed by different analytes of the sample of interest or viceversa, some calibration standards may suppress the signal of some analytes of interest. So the internal calibration standard should not interact with the sample in order to get a reliable mass spectra.^[23]

In this project, gold nanoparticles and red phosphorus will be evaluated as internal calibration standards for the analysis of HEK 293 in MALDI/SALDI TOF MS. Both elements are monoisotopic, thus, each cluster is represented only by one peak. Therefore, the mass spectra of these standards are simply to be analyzed.

1.5.1 Gold nanoparticles (AuNPs)

Gold nanoparticles (AuNPs) have caught lot of attention in different fields because of their unique physical and chemical properties which are due to the interaction of light with electrons on the gold surface at a specific wavelength. The wavelength at which this interaction occurs depends on the shape, size and surface area of the AuNPs. Therefore, considerable attention has been paid to the synthesis of these metal based nanostructures.^[24, 25]

Different approaches have been developed to synthesize AuNPs, but the chemical ones are the most used as they are low cost and easy to scale-up. These methods are usually done by reducing HAuCl_4 , with or without a capping reagent which helps controlling particle size and shape, preventing aggregation and improving function of the particle surface for different applications.^[26]

Gold nanoparticles have been used in many different fields, especially the medicine field in drug delivery, imaging, diagnosis and therapeutics,^[24] thus, their toxicity is an important factor to be considered. Several studies have been done regarding AuNPs cytotoxicity, but still there are some discrepancies.

Two different types of gold nanoparticles will be used in this project, flower-like gold nanoparticles (AuNF), and red gold nanoparticles (Red AuNPs), also called as polyhedral gold nanoparticles.

1.5.1.1 Flower-like gold nanoparticles (AuNFs)

Flower-like gold nanoparticles are highly branched nanometer-scale structures resembling a flower with a diameter of 40nm approximately.^[9, 27] (**Fig. 5**).

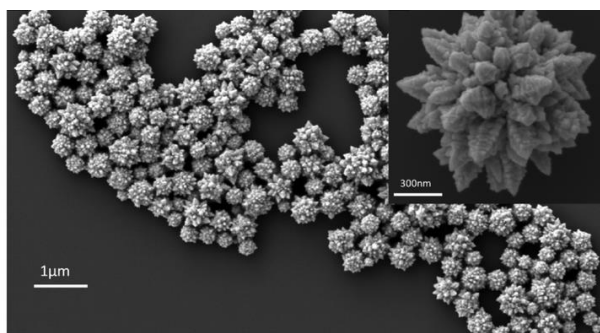


Figure 5. Scanning electron microscope images of AuNFs. Adapted from [28].

AuNFs have attracted much attention due to their highly branched shape which increases their surface, thus, making them suitable for bioimaging, biosensing, drug delivery and tissue engineering.^[27, 28]

The synthesis of AuNFs is quite challenging due to their complex 3-D structure. Different parameters such as temperature, concentration of the reducing agent and viscosity of the reaction solvent influence their size and shape.^[28]

1.5.1.2 Red gold nanoparticles (red AuNPs) or polyhedral gold nanoparticles

Red gold nanoparticles are three dimensional gold structures with polygon sides of approximately 90nm of diameter. They can gather into various polyhedral particles forming tetrahedrons, hexahedrons, octahedrons, etc.^[9] (**Fig. 6**)

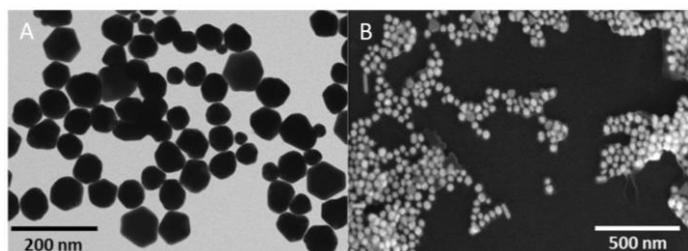


Figure 6. Polyhedral gold nanoparticles. **A)** transmission electron microscope image **B)** scanning electron microscope image. Adapted from [9].

Their synthesis is not as challenging as the flower-like gold nanoparticles. Their size and shape are controlled by the ratio of HAuCl_4 and the reducing agent. Some stabilizers such as high molecular weight polymers during their synthesis can also play an important role in determining their size and shape.^[26]

1.5.2 Red phosphorus

Phosphorus is a chemical element which can be found in various allotropes. The most common ones are red phosphorus, white phosphorus and black phosphorus. The former one will be the one used in this project as it has been stated that is not toxic, inert and monoisotopic.^[23]

Red phosphorus is formed by 4 tetrahedral (P_4) grouped phosphorus atoms. It can be synthesized by heating white phosphorus up to 300 °C which allows the formation of bonds between the P_4 forming a polymer (**Fig. 7**).^[29] The fact of forming a polymer makes red phosphorus more stable than white phosphorus.

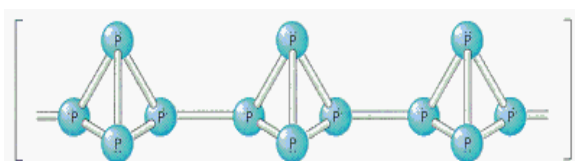


Figure 7. Red phosphorus structure. Adapted from [29].

Red phosphorus is used in the industrial sector in fireworks, pesticides, fertilizers etc.

Some studies have been done regarding the toxicity of phosphorus in plants and mammal cells when altering its homeostasis.^[30-32] But no studies have yet been done concerning the toxicity of red phosphorus when cultivated directly with cells. Thus, this project will also study the cytotoxicity of red phosphorus in HEK 293 cells.

1.6 HEK 293 cells

Human embryonic kidney cell line (HEK 293) were derived from transformation of kidney cells of an aborted embryo by adenovirus type 5 in 1973.^[33]

They are broadly used in cell biology, biotechnology and biomedical research because of their ease of growth and transfection.

In **Figure 8** it can be seen their adherent fibroblastoid morphology, growing as a monolayer.

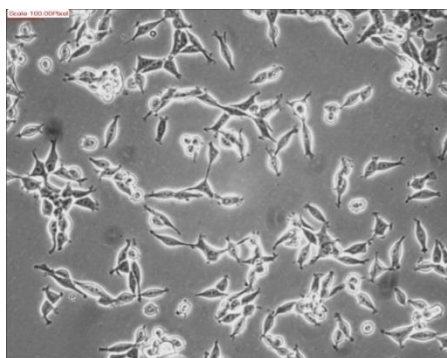


Figure 8. Optical microscope images of HEK 293 cells with 10x/0.4 magnitude and scale 100.00 pixel.

2. Objectives

This project will focus on:

- Determining whether flower-like gold nanoparticles, red gold nanoparticles and red phosphorus can serve as internal calibration standards for the analysis of cells by MALDI TOF MS.
- Determining if flower-like gold nanoparticles and red gold nanoparticles can be used as a matrix for SALDI TOF MS analysis.
- Study if these three components are toxic to cells in NP-uptake assays.

3. Methodology

HEK 293 cells were kept in high glucose (4.5 g / L) Dulbecco's modified eagle medium (DMEM) enriched with 10% of fetal bovine serum (FBS) and 1% of penicillin/streptomycin (full medium) and incubated at 37 °C in a humidified thermostat (thermo scientific) in 5% CO₂ atmosphere.

Pictures from the cells were taken from an inverted optical microscope (Nikon eclipse T5100).

Although HEK 293 cells contain part of a viral genome, they are categorized in the biosafety level 1 according to the central committee for biological safety, as they cannot release infectious virus particles.^[34] All the experiments with cells were done in a biosafety level 2 laboratory. No ethical issues were raised.

3.1 LDI/MALDI/SALDI TOF MS

All mass spectra were measured on AXIMA CFR TOF mass spectrometer (Kratos Analytical, Manchester, UK) equipped with a nitrogen laser (337 nm). Laser energy is specified in each spectra and expressed in arbitrary units (a.u.). All measurements were performed in a positive linear ion mode in a mass range 0-20000 kDa.

3.1.1 Treatments

Both gold nanoparticles and HEK 293 cells were analyzed by LDI TOF MS. See **Table 1**.

Table 1. Samples used for LDI TOF MS analyses.

Sample	Stabilizer	Ratio
AuNFs	CB	1:1
Red AuNPs	CB	1:1
AuNFs	-	-
Red AuNPs	-	-
Red phosphorus	-	-
HEK 293 cells	-	-

In order to analyze the different cell samples with SALDI TOF MS or MALDI TOF MS, cells were cultivated using different treatments shown in **Table 2** and **Table 3**, respectively.

Table 2. Treatments used for SALDI TOF MS analyses.

Cells	Cultivated (24h) with	Matrix	Ratio
HEK 293 cells	-	AuNFs (0.718 g / L)	2:1
HEK 293 cells	-	Red AuNPs (0.04727 g / L)	2:1

Table 3. Treatments used for MALDI TOF MS analyses.

Cells	Cultivated (24h) with	Matrix	Additional	Ratio
HEK 293 cells	-	SA (30 g / L)	-	2:1
HEK 293 cells	-	AuNFs (0.718 g / L) + SA (30 g / L) (1:1)	-	1:1
HEK 293 cells	-	Red AuNPs (0.04727 g / L) + SA (30 g / L) (1:1)	-	1:1
HEK 293 cells	-	SA (30 g / L)	AuNF (0.718 g / L) + CB (1:1)	2:1:1
HEK 293 cells	-	SA (30 g / L)	Red P (1 g / L)	2:1:1
HEK 293 cells	AuNFs (0.126 mg / L)	SA (30 g / L)	-	2:1
HEK 293 cells	Red AuNPs (0.0378 mg / L)	SA (30 g / L)	-	2:1
HEK 293 cells	Red P (0.16 g / L)	SA (30 g / L)	-	2:1

3.1.2 Sample preparation

1. Cells were cultured in a 5 mL dish in full medium and treated with the corresponding compounds.
2. After 24 hours, the medium was soaked away with an aspirator. The dish was washed with phosphate buffered saline (PBS) to make sure no medium remains were left.
3. In order to detach the cells, the cells were cultured with 600 μ L of trypsin (Biosera) for 3 minutes at the thermostat at 37°C.
4. Cells were counted using the Neubauer chamber by the classical method.
5. The corresponding volume containing 1 million cells was centrifuged at 2000 rcf during 3 min.
6. Cells were washed in 500 μ L PBS and centrifuged again at 2000 rcf for 3 minutes. The supernatant was soaked away.
7. All cells were mixed with ammonium bicarbonate buffer (ABC) in the ratio 10^6 cells / 10 μ L of ABC.
8. 10 μ L of the mixture above was mixed with the correspondent matrix.
9. 2 μ L of the solution was placed on each spot of the target and let dry at air temperature.
10. Finally 2 μ L of the additional component was placed on top of the dried solution in the target.

In case that no cells were present on the sample, step number 9 was followed.

3.1.3 Reagents

3.1.3.1 Synthesis of flower-like gold nanoparticles (AuNFs)

AuNF were synthesized according to Jiang *et al.*,^[35] as it is a simple and low-cost method. 400 μ L of 1 M triethanolamine (Merck), was used to reduce 200 μ L of 25 mM HAuCl₄ (Sigma Aldrich), in 20 mL of pure ethylene glycol (Lachema) as a reaction solvent. The final concentration was 0.718 g Au / L in distilled water.

Although, neither triethanolamine or ethylene glycol are environmentally toxic according to the regulation (EC) No 1272/2008 their release on the environment should be avoided.^[36, 37]

3.1.3.2 Synthesis of red gold nanoparticles (red AuNPs)

Red gold nanoparticles were synthesized according to Wang *et al.*^[26]

800 μ L of 1M gallic acid (Sigma Aldrich), was used to reduce 3.2 mL of 0.3mM HAuCl₄ (Sigma Aldrich). The final concentration was 0.04727 g Au / L in distilled water.

Although gallic acid is not environmentally toxic according to the regulation (EC) No 1272/2008 its release on the environment should be avoided.^[38]

3.1.3.3 Synthesis of red phosphorus (red P)

Red phosphorus derives from white phosphorus. The latter, is hazardous not only for the health but also for the environment.^[29] Red P was obtained from the department of analytical chemistry of Masaryk university which accomplishes the required conditions for the handling of white phosphorus.

For cultivating with cells: 1 μ g of red phosphorus (Riedel de Haën) was dissolved in 1 μ L of distilled water.

As a matrix: 1 μ g of red phosphorus (Riedel de Haën) was dissolved in 1 μ L of acetonitrile (Merk).

3.1.3.4 Sinapinic acid (SA)

Sinapinic acid was used as a matrix for MALDI TOF MS. It was prepared in a final concentration of 30 mg / mL in 70% acetonitrile (Merk), 7.5% of trifluoroacetic acid (Sigma Aldrich) and 22.5% of distilled water.

3.1.3.5 Ammonium bicarbonate (ABC)

A 150 mM ammonium bicarbonate (Sigma Aldrich) solution was used to resuspend the cell pellet.

3.1.3.6 Citrate buffer (CB)

Citrate buffer consisted of 7.5 mM triammonium citrate (Sigma Aldrich) and 5 mM of citric acid (Penta). It was used to stabilize gold nanoparticles and getting more gold clusters in the mass spectra.

3.2 MTT assay

3.2.1 Cultivation of cells for the MTT assay

An MTT experiment was done in order to analyze the cytotoxicity of gold nanoparticles. The treatments used are shown in **Table 4**.

Table 4. Treatments used for MTT assay.

Cells	Cultivated (24 h) with
HEK 293 cells	-
HEK 293 cells	AuNFs (0.252 mg / L)
HEK 293 cells	Red AuNPs (0.0756 mg / L)

1. 25000 HEK 293 cells were seeded in pentaplicate on a 96-well plate in a final volume of 200 μ L and incubated in the thermostat for 4 hours to allow attachment.
2. Cells were treated for 24 hours with the correspondents gold nanoparticles.
3. 20 μ L of MTT was added and incubated for 3 hours in the thermostat.
4. Medium was replaced by 100 μ L of detergent to lyse the cells.
5. Absorbance was measured at 570 nm with Synergy HTX spectrophotometer.

3.2.2 Reagents

3.2.2.1 MTT reagent

10x of MTT was used: 50 mg of thiazolyl blue tetrayolium bromide (Sigma Aldrich) dissolved in 5 mL of distilled water. It was stored at -20 $^{\circ}$ C.

3.2.2.2 Detergent

The detergent was used to lyse the cells so that the reduced MTT salt (formazan) could be measured by an spectrophotometer. Its components are 10% triton/tween (Sigma Aldrich), 90% isopropanol (Penta) and 0.04 M HCl.

3.3 Growth curve

3.3.1 Cultivation of cells for the growth curve

A growth curve was measured for cells treated with phosphorus to study its cytotoxicity. The different treatments are shown in **Table 5**.

Table 5. Treatments used for doing the growth curve of HEK 293 cells treated with phosphorus.

Cells	Cultivated (24 h) with
HEK 293 cells	-
HEK 293 cells	Red P (0.1667 g / L)
HEK 293 cells	Red P (0.333 g / L)

1. 500000 cells were seeded in triplicates on a 5 mL dish.
2. Every 24 hours cells were detached from the dish, put in a tube with medium and counted following the same steps as mentioned on section 3.1.2 (point 1-4)

4. Results

HEK 293 cells were used to study the potential of gold nanoparticles and red phosphorus to be used as internal calibration standards in MALDI TOF MS analyses. The same cells were also used to study the enzymatic and chemical modifications AuNPs and red P may induce in their cytoplasm. Thus, one of the first samples to be measured by MALDI TOF MS technique was HEK 293 cells with sinapinic acid as a matrix (**Fig. 9 (A)**). This sample will also be referred as the control.

AuNFs are possible candidates to be used as internal calibration standards for cells in MALDI TOF MS analyses

First of all, AuNFs and red AuNPs stabilized by citrate buffer were measured using LDI TOF MS technique (**Fig. 9 (B), (C)**). Well-defined gold clusters in the range 1000-6000 m/z were present, being AuNFs spectrum the one with more intense peaks.

Next step was to mix both gold nanoparticles with HEK 293 using sinapinic acid as a matrix, but only the peaks corresponding to cell organic compounds had been seen in the mass spectra (**Fig. 9 (D), (E)**). Therefore, the following sample measured was a mixture of matrix with both AuNPs (**Fig. 9 (G,H)**) to see if sinapinic acid (SA) interacted with gold shielding its clusters in the mass spectra. No gold clusters could be seen, only matrix clusters (marked with an asterisk) and other peaks were observed. The peaks marked in orange (**Fig. 9 G, H**) may correspond to the interactions between the gold and SA with their possible structure on the right of the Figure confirming that sinapinic acid interacted with gold. The next attempt was to repeat the experiments without using matrix. By doing so, we were not only studying if AuNPs could be used as internal calibration standards but also if they would be a good matrix for SALDI TOF MS technique. Firstly, HEK 293 cells without any matrix were measured (**Fig. 10 (A)**), the mass spectra were recorded in the m/z range 0 to 300 m/z . Following on, it was confirmed that gold clusters of AuNFs and red AuNPs without using any matrix or stabilizer can be observed in the mass spectra (**Fig. 10 (B,C)**), being the clusters of the latter more intense. This may be due to the fact that when no stabilizer is used, the 3-D structure of red AuNPs is more resistant to the laser beam than the highly branched 3-D structure of AuNFs. Finally, the mass spectra of cells mixed with gold nanoparticles (without matrix) were obtained up to a m/z of 1000 (**Fig. 10 (D,E)**). The first five gold clusters as well as the peaks around 81 m/z , 86 m/z , 97 m/z , 113 m/z , 125 m/z , 141 m/z and 157 m/z could be seen in the mass spectra. These peaks were also present in the mass spectra depicted in **Figure 10 (A)**. So we conclude that they correspond to the low molecular organic compounds of HEK 293 cells.

In the spectrum obtained mixing HEK 293 with red gold nanoparticles, 3 additional peaks can be seen: 296 m/z , 312 m/z and 420 m/z . These peaks are also present in the mass spectra of control cells (**Fig. 9 (A)**). However, they are not labeled in the spectra due to the fact they are not reproducible and their intensities are lower than 1mv.

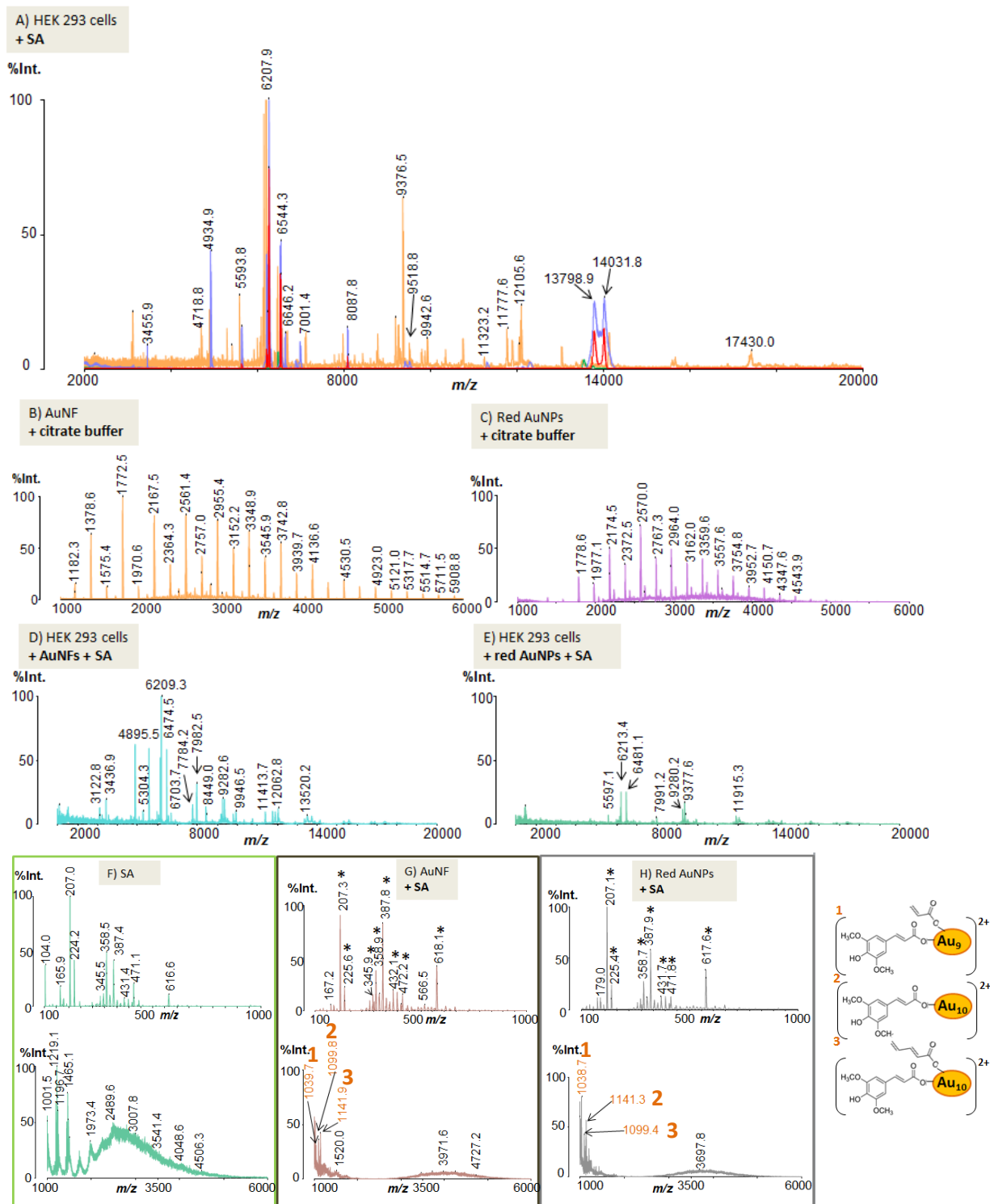
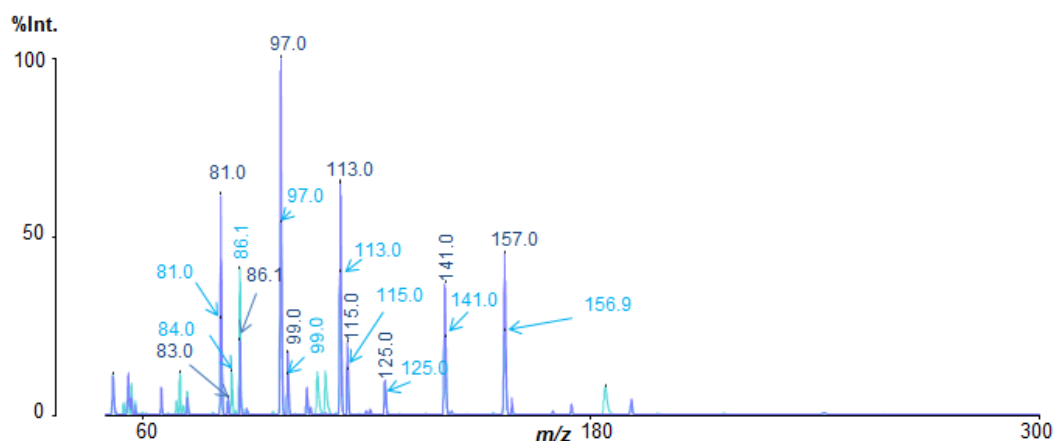
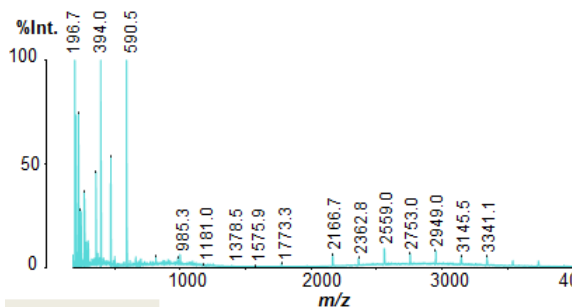


Figure 9. A) Four independent mass spectra of HEK 293 cells using sinapinic acid as a matrix superposed. These four mass spectra were externally calibrated with red phosphorus. The labeled peaks are present in at least 2 of the 4 spectra. B) Mass spectrum of AuNFs stabilized by citrate. The mass spectrum was calibrated with a tolerance 100 mDa using Na, K and gold clusters of known mass (Au₁, Au₆, Au₇, Au₁₁, Au₄₇, Au₄₈). C) Mass spectrum of red AuNPs stabilized by citrate buffer. The mass spectrum was calibrated with a tolerance of 200 mDa using Na, K and gold clusters of known mass (Au₁-Au₃, Au₅, Au₁₇, Au₁₈). D) Mass spectrum of HEK 293 cells mixed with AuNFs and sinapinic acid as a matrix. The mass spectrum was externally calibrated by red phosphorus. E) Mass spectrum of HEK 293 cells mixed with red AuNPs and sinapinic acid as a matrix. The mass spectrum was externally calibrated by red phosphorus. F) Mass spectrum of sinapinic acid. G) Mass spectrum of AuNFs mixed with SA as a matrix. H) Mass spectrum of Red AuNPs mixed with SA as a matrix. Profile scale of spectrum C was relative to spectrum B. Profile scale of spectrum D and E were relative to spectra A. The measurements were performed with a laser power of A: 105-115 a.u.; B and C: 164 a.u.; D, E, G and H: 115 a.u.; F: 130 a.u.

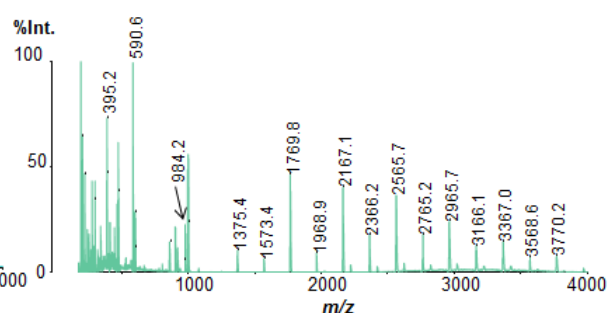
A) Hek 293 cells



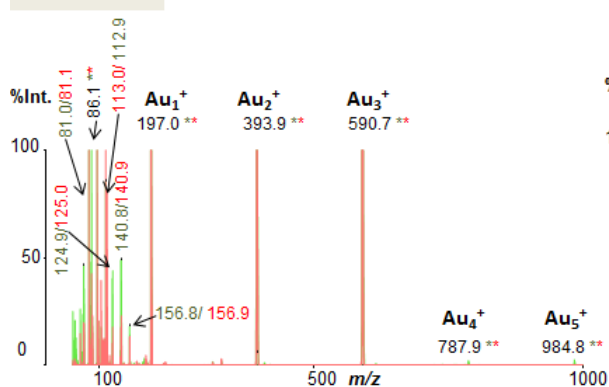
B) AuNFs



C) Red AuNPs



D) Hek 293 cells + AuNFs



E) Hek 293 cells + red AuNPs

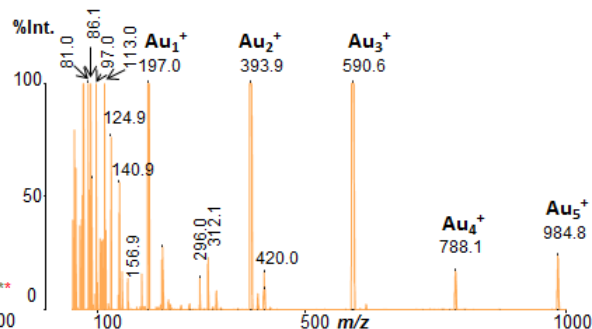


Figure 10. **A)** Two independent mass spectra of HEK 293 cells without using any matrix superposed. Both spectra were externally calibrated with red phosphorus. **B)** Mass spectrum of AuNFs without any matrix or stabilizer. The mass spectrum was calibrated with a tolerance of 500 mDa using Na, K and gold clusters of known mass (Au_1 , Au_2 , Au_3 , Au_7 , Au_{13} , Au_{16} , Au_{17}). **C)** Mass spectrum of Red AuNPs without any matrix or stabilizer. The mass spectrum was calibrated with a tolerance of 500 mDa using Na, K and gold clusters of known mass (Au_1 , Au_2 , Au_4 , Au_{11} , Au_{12} , Au_{13}). **D)** Two independent mass spectra of HEK 293 cells mixed with AuNFs as the only matrix superposed. Both mass spectra were calibrated with a tolerance of 300 mDa using Na, K and gold clusters of known mass (Au_1 , Au_2 , Au_3 , Au_4 and Au_5). **E)** Mass spectrum of HEK 293 cells mixed with Red AuNPs as the only matrix. The mass spectrum was calibrated with a tolerance of 300 mDa using Na, K and gold clusters of known mass (Au_1 , Au_2 and Au_3).

Profile scale of spectrum **B** was relative to spectrum **C**. Profile scale of spectra **D** and **E** were relative to spectra **A**. The measurements were performed with a laser power of **A**: 115-130 a.u.; **B**: 132 a.u.; **C**, **D** and **E**: 130 a.u.

Finally, a last approach was tested in order to get a better spectrum where gold and HEK 293 organic compounds would be seen at higher intensities and m/z range. The procedure tested consisted of mixing HEK 293 cells with sinapinic acid and let to dry, once the mixture was crystallized, flower-like

gold nanoparticles stabilized by citrate buffer were added on the top. Although the spectrum obtained had a high background noise, gold clusters at a low m/z range and HEK 293 organic compounds at a high m/z range could be seen. (**Fig. 11**). Sinapinic acid clusters could also be seen at a low m/z range.

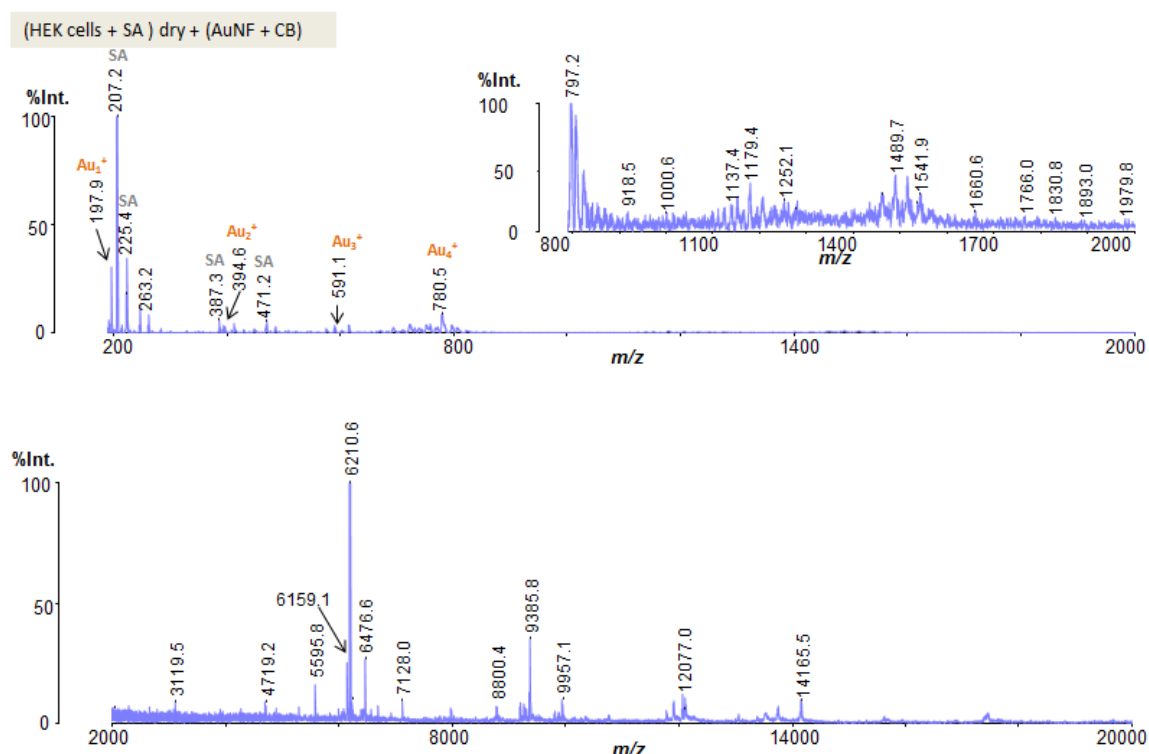


Figure 11. Mass spectrum of HEK 293 cells crystallized with sinapinic acid with AuNF stabilized by citrate buffer on top. The spectrum was externally calibrated with red phosphorus. The measurement was performed with a laser power of 105 a.u. The profile scale of the mass spectrum was relative to the control cells.

AuNFs produce a shift in the MS of treated cells

In order to study the enzymatic or chemical modifications that AuNPs can induce in the HEK 293 cytoplasm, we had cultivated these cells with both AuNPs for 24 hours. No significant changes in cell density were observed (**Fig. 12**).

Moreover, we performed an MTT assay to obtain quantitative results concerning the viability and proliferation of cells when they were cultivated with AuNPs (**Fig. 13**). The results show that, within the value of standard deviation, no significant changes between the absorbance of each treatment were obtained. A Student T test was also performed assuming that the data followed a parametric distribution. The calculated α -error between control cells and treated cells with AuNFs and red AuNPs was of 0.22 and 0.83, respectively, confirming that there are no significant differences between control cells and AuNPs treated cells.

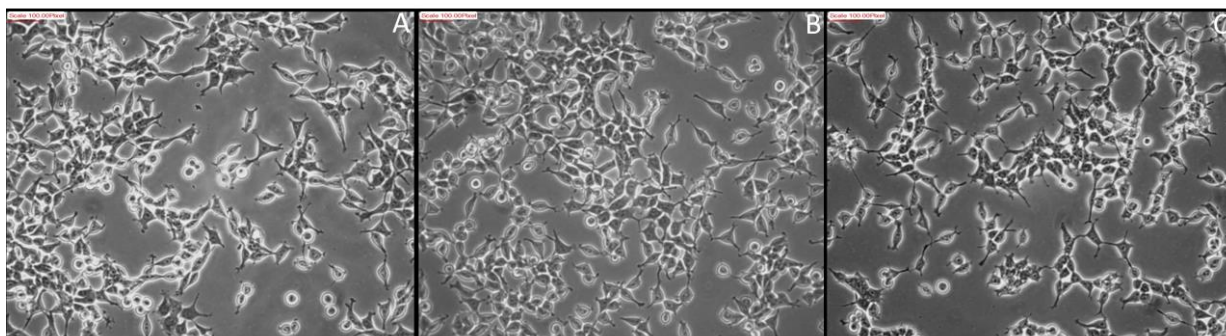


Figure 12. Optical microscope images with 10x/0.40 magnitude and scale 100.00 pixel. **A)** HEK 293 cells. **B)** HEK 293 cells cultivated 24 h with 0.126 mg / L AuNFs. **C)** HEK 293 cells cultivated 24 h with 0.0378 mg / L red AuNPs.

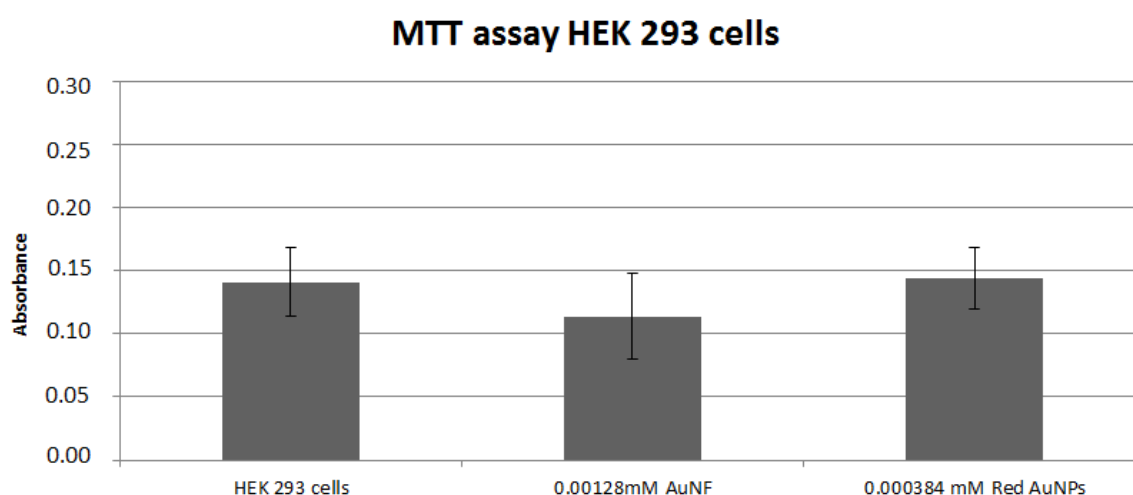


Figure 13. Results from MTT assay. Absorbance was recorded at 570 nm. The plot shows the means and the standard deviations (SD) of 5 replicates.

Further analysis were done to asses macromolecular content differences between control and AuNPs cultivated cells by comparing their MALDI TOF MS mass spectra (**Fig. 14**).

Only one difference was observed. In the case of the cells cultivated with flower-like gold nanoparticles, the intensity of the peak around 6550 m/z was lower than the peak around 6650 m/z whereas the opposite was observed in the mass spectra depicted in **Figure 9 (A and D)**. However, this shift was not observed in the mass spectra of cells cultivated with red gold nanoparticles (**Fig. 14 (B)**).

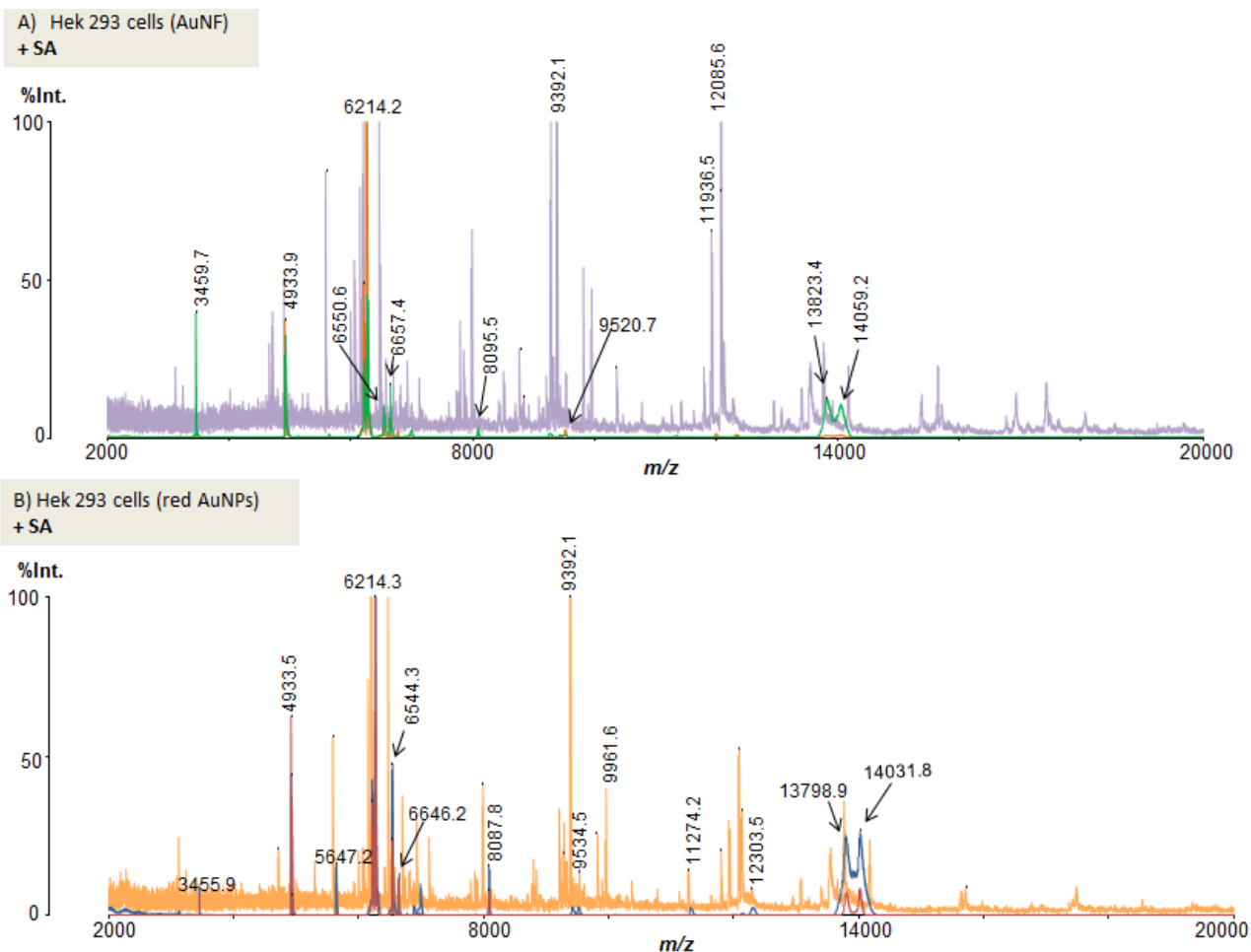


Figure 14. A) Three independent mass spectra of HEK 293 cells cultivated with AuNFs using sinapinic acid as a matrix superposed. **B)** Three independent mass spectra of HEK 293 cells cultivated with red AuNPs using sinapinic acid as a matrix. All spectra were externally calibrated with red phosphorus. The measurements were performed with a laser power between 105-115 u.a. The profile scale of both mass spectra were relative to control cells. The labeled peaks were present in at least 2 of the 3 spectra superposed.

Red P is a possible candidate to be used as internal calibration standard for cells in MALDI TOF MS analyses

Clear odd phosphorus clusters were seen either by laser desorption/ionization of red phosphorus (**Fig. 15 (A)**) and by matrix assisted laser desorption/ionization of a mixture of red phosphorus with HEK 293 cells already crystallized with sinapinic acid (**Fig. 15 (B)**). Over a 2600 m/z , the intensity of the peaks in **Figure 15 (A)** is zero, whereas in **Figure 15 (B)**, some other peaks corresponding to HEK 293 organic compounds can be seen at higher m/z ranges. These peaks are shifted from the peaks seen in the mass spectra of control cells (**Fig. 9 (A)**).

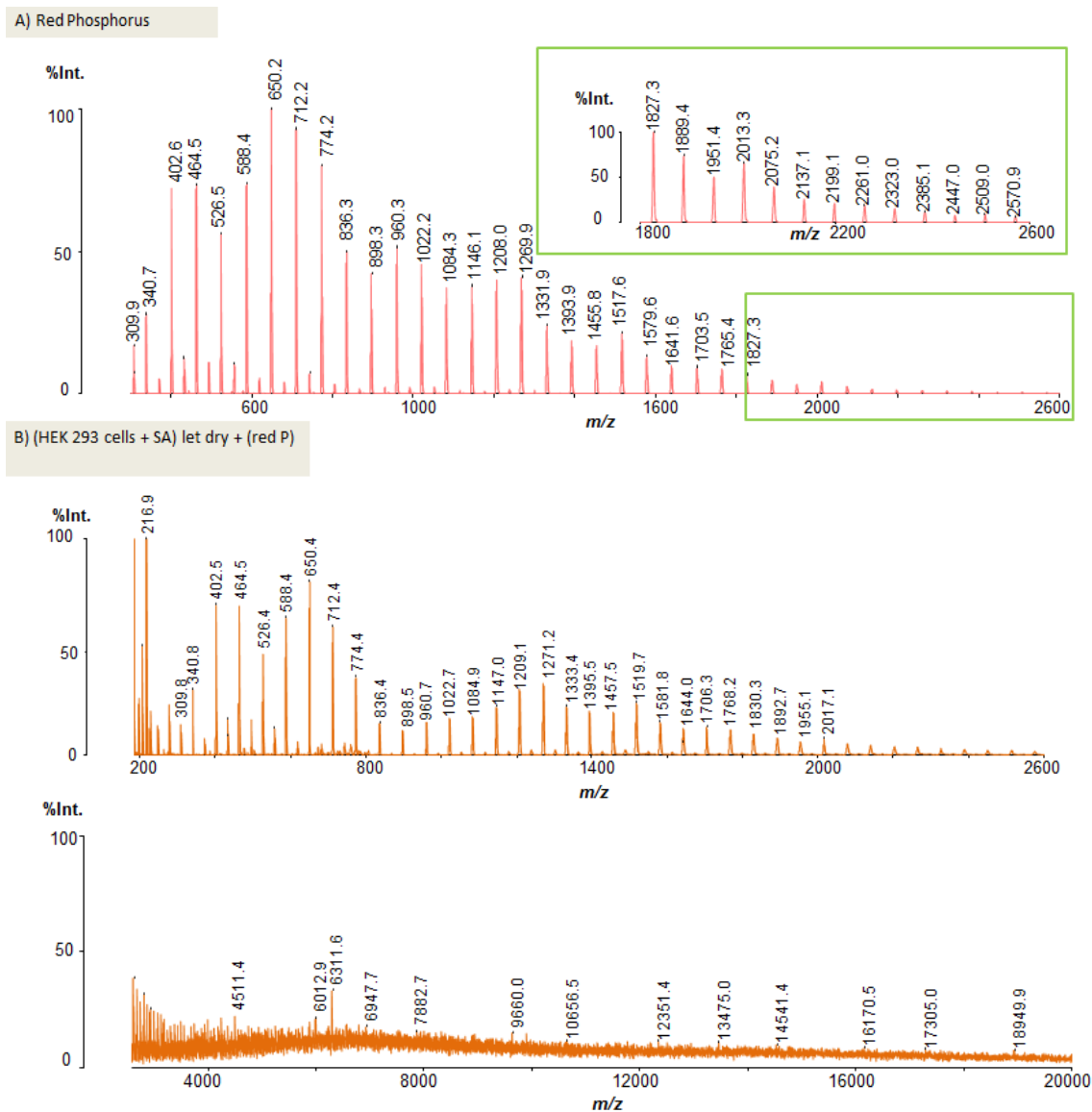


Figure 15. A) Mass spectrum of red phosphorus. The mass spectrum was calibrated with a tolerance of 200mDa using odd phosphorus clusters of known mass (P_3 - P_{95} , P_{101} - P_{109} , P_{115} - P_{133}). **B)** Mass spectrum of HEK 293 cells crystallized with sinapinic acid and adding red P on top. The mass spectrum was calibrated with a tolerance of 200mDa using Na, K and odd phosphorus clusters of known mass (P_5 - P_{27} , P_{53} , P_{69} , P_{73} , P_{75} and P_{83}). The profile scale of spectrum **B** was relative to the control mass spectrum. The measurements were performed with a laser power of **A**: 126 a.u.; **B**: 135 a.u.

Red P inhibits cell growth and proliferation

Cells were cultivated for 24 hours with red phosphorus. Apparently, no significant differences in cell density were observed (**Fig. 16**). Notice that the black spots in **Figure 16 (B)** are aggregates of red phosphorus.

A growth curve was done in order to get quantitative results about cell viability and proliferation (**Fig. 17 (A)**). It can be observed that the highest the concentration of red phosphorus and the longest the cultivation time with the element, the highest the inhibition of cell growth and proliferation. The Student T test was calculated as well, assuming that the data followed a parametric distribution (**Fig.**

17 (B)). The differences between control cells and cells treated with 0.166 g / L of P were no relevant; this is the reason why cell density differences cannot be observed in **Figure 16**. However, the differences between control cells and cells treated with 0.333 g / L were significant.

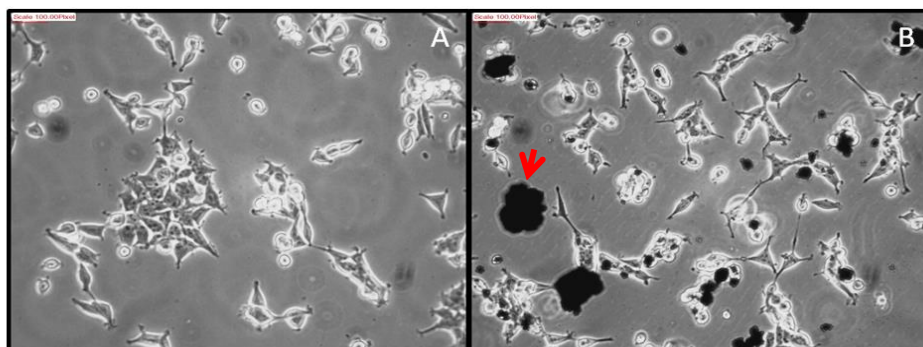


Figure 16. Optical microscope images with 10x/0.40 magnitude and scale 100.00 pixel. **A)** HEK 293 cells. **B)** HEK 293 cells cultivated 24h with 0.1666 g / L of red phosphorus. The red arrow shows an aggregate of red phosphorus.

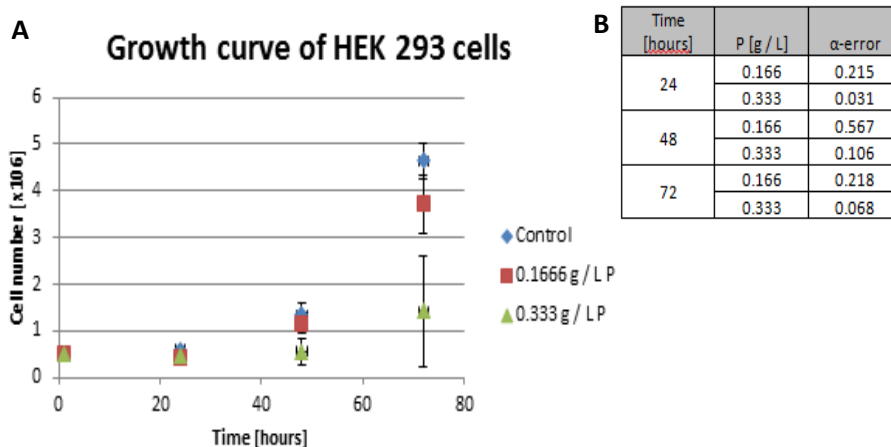


Figure 17. A) HEK 293 growth curve without treatment (blue), cultivated with 0.1666 g / L red P (red) and cultivated with 0.333 g / L red P (green). The plot shows the means and the standard deviations (SD) of two independent experiments. **B)** Student T test of each treatment in respect to control.

Further analyses were performed using MALDI TOF MS to see if there were differences between the mass spectra of cells cultivated with red phosphorus with respect to non-treated cells (**Fig. 18**).

Although it cannot be observed in **Figure 18**, the intensity of the mass spectrum peaks of the cells cultivated with red phosphorus was very low at high m/z ranges, being the maximum 0.1mV. This is the reason why the profile scale is relative to the highest peak and not to the control because if we did so, these peaks cannot be observed.

Due to the low intensity and to the high background noise, at a high m/z range, only 3 peaks (5652.1 m/z , 6552.1 m/z and 13850.5 m/z) can be observed in the spectrum of HEK 293 cells cultivated with red phosphorus (**Fig. 18, red**). These peaks could be correlated with the peaks (5295.0 m/z , 6311.6

m/z and 13475.0 m/z) observed in the mass spectrum of HEK 293 cells crystallized with sinapinic acid and with red phosphorus on top (**Fig. 18, blue**).

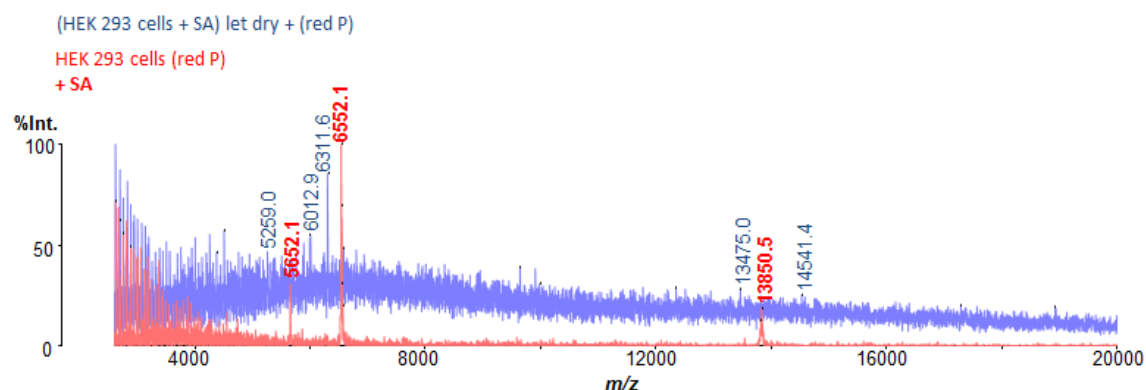


Figure 18. Comparison of the mass spectrum of cells cultivated with red phosphorus (red spectrum) and cells crystallized with sinapinic acid with red phosphorus on top (blue spectrum). The mass spectrum of HEK 293 cells cultivated with red phosphorus was calibrated with a tolerance of 100 mDa using Na, K and odd phosphorus clusters of known mass (P_3 - P_7 , P_{11} - P_{15} , P_{27} - P_{41} , P_{45} and P_{47}). The measurement was performed with a laser power of 132 u.a. The profile scale of both spectrum is relative to the highest peak in each spectrum.

5. Discussion

In this study, we found that flower-like gold nanoparticles (AuNFs) and red phosphorus (Red P) are promising internal calibration standards for HEK 293 cells in matrix assisted laser desorption/ionization (MALDI). The most appropriate methodology to use these standards, which still needs to be improved, seems to be letting crystallize the sample with sinapinic acid (SA) and then adding AuNFs stabilized by citrate buffer or Red P on top, respectively.

There was not enough time to study the capability of red gold nanoparticles (Red AuNPs) to be used as internal calibration standards for cells following the methodology explained above.

What prompted us to study if AuNPs could be used as internal calibration standards for MALDI TOF MS measurements of cells, was the distinct monoisotopic gold clusters obtained in the mass spectra (MS) by laser desorption/ionization (LDI) of AuNFs and red AuNPs stabilized by citrate buffer (**Fig. 9 (B, C)**).

Moreover, it was recently stated that AuNFs can be used as an internal calibration standard for peptides in SALDI TOF MS analyses.^[9] However, it is necessary to evaluate their capability in order to be used as internal calibration standards for complex samples, such as intact cells, in MALDI TOF MS analyses.

In our approach, the interaction between the matrix and AuNPs was reduced by letting crystallize sinapinic acid with the cells. This interaction was evident in **Figure 9 (D,E)** (were no gold clusters can

be seen in the mass spectra) and proved in **Figure 9 (G,H)**. Sinapinic acid clusters were abundant at low m/z ranges impeding low molecular compounds peaks to be seen in MALDI TOF MS measurements, this drawback has already been stated in many papers.^[5, 9, 10] Interestingly, at m/z ranges between 1000 and 1200 we have observed three peaks corresponding to SA-AuNPs interactions (marked in orange in the mass spectra) already reported by Chen *et al.*^[39] Unfortunately, due to the low resolution of the mass spectra we could not demonstrate that these peaks had a charge of 2, thus, we could not confirm that they corresponded to the same SA-AuNPs interactions reported in this article.^[39]

In addition to sinapinic acid, α -cyano-4-hydroxycinnamic acid (CHCA) and 2,5-dihydroxybenzoic acid (DHB) are the most common matrices used in the analysis of proteins by MALDI.^[3] None of them would suit as a matrix to achieve our aim, as when mixing them with AuNPs gold clusters are neither seen in the mass spectra.^[40, 41]

However, even though MALDI matrices hinder our aim (since they shield gold clusters in the mass spectra), the alternative cannot be to not use them because AuNPs are not able to enhance the ionization of HEK 293 organic compounds at high m/z ranges as can be observed in **Figure 10 (D, E)**. Thus, gold nanoparticles are not suitable as SALDI matrices and calibration standards in complex samples such as cells.

Furthermore, we realized that gold clusters in LDI mass spectra of both AuNPs (**Fig. 10 (B, C)**) were less intense and in lower amount than those obtained in the presence of citrate buffer in **Figure 9 (B,C)**. This fact was also observed by Kolářová *et al.*, which suggested that the stabilizing effect of citrate buffer is necessary for the formation of higher gold clusters of both AuNPs.^[9]

Following the developed methodology, we failed in obtaining the peaks of high HEK 293 organic compounds together with the peaks of gold clusters at the same m/z range, as gold clusters only appeared up to 800 m/z (**Fig. 11**). Thus, the methodology should be optimized to obtain gold clusters at higher m/z ranges in the mass spectra. So, AuNPs cannot be used for calibrating high m/z HEK 293 organic compounds. A possible approach would be by increasing the laser energy as Kolářová *et al.* observed in the case of gold clusters that their ionization was enhanced by increasing laser energy.^[9]

Red P presents, as well as AuNPs, well-defined monoisotopic clusters in LDI mass spectrum that can be used as an external calibration standard for cells. Red phosphorus was reported to be a good internal calibration standard for peptides^[23] but its capability to be used as an internal calibration standard in the MS analysis of intact cells has not yet been explored.

Applying the above described methodology (adding red P on top of the cells previously crystallized with SA), we obtained high and intense phosphorus clusters peaks together with high HEK 293 organic compound peaks in the mass spectrum (**Fig. 15 (B)**) even though, shifted from the ones that we observed in the control mass spectra (**Fig. 9 (A)**). Therefore, we cannot exclude the existence of possible interactions between red P and HEK 293 organic compounds. This fact has to be taken into account and further clarified. The experiment should be repeated, and the methodology used improved since the background noise in the mass spectrum was relatively high and not enough phosphorus clusters could be seen (just up to 26000 m/z) to calibrate high HEK 293 organic compounds (2000-20000 m/z) (**Fig. 15 (B)**).

Besides studying the use of AuNPs and red P as suitable internal calibration standards, we also studied their cell toxicity. The results show that cell viability and proliferation were not affected by AuNPs. However, in the case of red phosphorus, these cell parameters were altered in a dose dependent manner. Moreover, we determined that the size and shape of gold nanoparticles affected both cell response and MALDI ionization effects.

What prompted us to study gold cytotoxicity is the fact that gold nanoparticles are of quite interest in the medical field, thus, studying the enzymatic or chemical modifications that AuNPs will induce on the cell cytoplasm is of major importance.

Results about the cytotoxicity of AuNPs differ from each study. On one hand, some articles state that AuNPs do not produce any negative effects,^[42-44] whereas in others, it is remarked that AuNPs trigger the apoptotic pathway by induction of oxidative stress, endoplasmic reticulum stress or degradation of cytoskeletal proteins, etc.^[45-47]

In our study, we did not find significant differences between treated and non-treated cells regarding to cell viability and proliferation when performing an MTT assay (**Fig. 13**). The basis of this assay is that the reduction of the MTT salt to formazan by mitochondrial enzymes is directly proportional to the number of living cells.^[48]

The fact that, in our study, cell viability and proliferation were not affected by AuNPs is explained by the relatively low concentration of AuNPs used in our experiments in comparison to the concentration used in other studies. For instance, Noël *et al.*,^[45] Ramalingam *et al.*^[46] and Mateo *et al.*^[47] found a significant increase in apoptosis of polymorphonuclear neutrophil cells, A549 cells and human dermal fibroblast by using 400, 50 or 100 times, respectively, the concentration of AuNPs used in our study. Thus, assuming that the contradictory results found in the literature are mainly due to the different conditions used in each study (cell type, concentration of AuNPs, cultivation period, type of assay, etc.).

Many of the studies regarding gold cytotoxicity found in the literature, are based in colorimetric methods (MTT and lactate dehydrogenase assay (LDH)) or fluorescent methods (reactive oxygen species assays (ROS), real-time polymerase chain reaction (RT-PCR)), DNA microarray analyses, etc.). Although these techniques are widely used to assess other drugs cytotoxicity, an important issue to be considered is the fact that AuNPs absorb in the visible region and thus, can interfere in the measurements. Therefore this issue needs to be carefully controlled.^[49]

Considering the drawbacks for colorimetric and fluorescent methods, we proposed MALDI TOF MS as the most appropriate technique for studying the changes induced by AuNPs on the macromolecular content of the cells. Moreover, analyzing the mass spectra would enable us to distinguish which signaling pathways are up/down-regulated in treated cells by looking at the intensity of the peaks in the mass spectrum. Therefore, it would enable us to determine, for example, if cell death is due to natural causes or induced by AuNPs triggering other apoptotic pathways.

Though the spectra obtained in **Figure 14** were not clear enough to make some conclusions, we saw a shift regarding the intensity ratios in the mass spectra of cells cultivated with AuNFs (**Fig. 14 (A)**)

that was not seen in the mass spectra of non-treated cells (**Fig. 9**). Interestingly, this shift was not observed in the mass spectra of cells cultivated with red AuNPs (**Fig. 14 (B)**). This can be due to the fact that AuNFs and red AuNPs differ in size and shape. It is known that cellular uptake of AuNPs is influenced by their geometry.^[50] Thus, cell response will be affected in a different manner depending on the concentration of gold inside the cells. However, it has also been found in literature that ionization of small peaks is enhanced by AuNFs in MALDI TOF MS.^[9] Although we cannot determine if this shift is related to a cytotoxicity effect or to a MALDI ionization effect of AuNFs, we can conclude that the shape and the size of AuNPs is an important issue to take into account in studying the cytotoxicity of AuNPs.

Additional studies controlling the AuNPs conditions (concentration, size, shape, etc.) should be performed in vivo and in vitro to determine their toxicity dosage, their effects on cells and the interaction with other components. In the case of in vivo experiments, to get more reliable results about cytotoxicity of AuNPs. Further studies should also be done regarding the performance of MALDI TOF MS analyses in order to improve resolution of the mass spectra.

Even though Red phosphorus is not as widely used as gold nanoparticles, we also studied its cytotoxicity. The fact that red phosphorus absorbs at the same wavelength as formazan (570 nm),^[51] unable the use of an MTT assay as red phosphorus would interfere with the signal, hence altering the results. As an alternative, a growth curve and an analysis by MALDI TOF MS were done. For the former approach we noticed that the highest the concentration of phosphorus, the more it inhibited cell growth and proliferation (**Fig. 17**). In fact, this finding was already reported, and growth inhibition, senescence and apoptosis in cells by altering the homeostasis of phosphorus in plants or mice were also observed.^[30-32] For the latter approach, no differences in the mass spectra of control cells and treated cells were observed (**Fig. 18**), probably due to the low intensity and the high background noise in the mass spectra.

Further studies should be done regarding the MALDI TOF MS analyses because maybe by getting clearer mass spectra with less background noise and more define peaks would enable us to see more changes in the macromolecular content between treated and non-treated cells.

At last, I would like to give a thoughtful analysis to the whole project regarding its ethics and sustainability.

The main aim of the project, studying the use of AuNPs and red P as internal calibration standards for HEK 293 cells analyses by MALDI TOF MS, was feasible, as other studies had already demonstrated their use as internal calibration standards for peptides in SALDI and MALDI TOF MS analyses, respectively. Moreover, this study would not only be a basic research driven by our interests but it would also be useful in applied research in obtaining very precise mass spectra needed, for example, in peptide mass fingerprinting. One of the potential applications of mass fingerprinting technique is the identification of proteins that are deregulated in an unhealthy person. Identifying these proteins is one of the first steps in order to understand a disease and find its cure. Thus, by studying AuNPs and red P as internal calibration standards for cell analyses by MALDI TOF MS, we may indirectly contribute to the society healthcare field.

Though the success of AuNPs or red P as internal calibration standards was not entirely realized, as no gold or phosphorus clusters peaks were observed up to 20000 m/z , the methodology is promising. By making further studies to improve the method it may be possible to achieve our aim.

Regarding the consequences this project may have on the environment, the main problematic issue is obtaining AuNPs and red P. As it is already mentioned in the methodology, the compounds used to obtain both AuNPs were not potentially toxic to the environment. However, red P was obtained from white P, which is hazardous not only to health but also to the environment. Therefore, the use of AuNPs as internal calibration standards might be more eco-friendly than using red P.

6. Conclusions

This study has demonstrated that flower-like gold nanoparticles and red phosphorus are promising compounds to be used as internal calibration standards when adding them on top of cells already crystallized with sinapinic acid. Using this methodology, the ionization of HEK 293 organic compounds is enhanced but at the same time the interaction between AuNFs or Red P with the matrix is diminished.

AuNFs and red AuNPs were not found suitable as a matrix for simultaneous calibration in SALDI TOF MS technique as they were not able to enhance the ionization of high molecular organic compounds of HEK 293.

Finally we studied the cytotoxicity of both elements in cells, determining that AuNPs were not toxic whereas red phosphorus affected negatively to cell viability and proliferation. We also found that AuNPs size and shape is an aspect to be considered not only in cytotoxicity studies but also in MALDI ionization effects.

7. References

- [1] Premierbiosoft.com. (2016). *Mass Spectrometry :: Introduction, Principle of Mass Spectrometry, Components of Mass Spectrometer, Applications*. [online] Available at: http://www.premierbiosoft.com/tech_notes/mass-spectrometry.html [Accessed 16 Apr. 2016].
- [2] Thermofisher.com. (2016). *Overview of Mass Spectrometry | Thermo Fisher Scientific*. [online] Available at: <https://www.thermofisher.com/cz/en/home/life-science/protein-biology/protein-biology-learning-center/protein-biology-resource-library/pierce-protein-methods/overview-mass-spectrometry.html.html> [Accessed 16 April 2016].
- [3] Hoffmann, E., Charette, J. and Stroobant, V. (2001). *Mass spectrometry*. New York: Wiley.
- [4] Selectscience.net. (2016). *Mass Spectrometry Buying Guide*. [online] Available at: http://www.selectscience.net/mass_spectrometry_buying_guide.aspx [Accessed 18 April 2016].
- [5] Peterson, D. (2006). Matrix-free methods for laser desorption/ionization mass spectrometry. *Mass Spectrom. Rev.*, 26(1), pp.19-34.
- [6] Siuzdak, G. (1994). The emergence of mass spectrometry in biochemical research. *Proceedings of the National Academy of Sciences*, 91(24), pp.11290-11297.

- [7] Szajli, E., Feher, T. and Medzihradsky, K. (2008). Investigating the Quantitative Nature of MALDI-TOF MS. *Molecular & Cellular Proteomics*, 7(12), pp.2410-2418.
- [8] Tholey, A. and Heinzle, E. (2006). Ionic (liquid) matrices for matrix-assisted laser desorption/ionization mass spectrometry—applications and perspectives. *Anal Bioanal Chem*, 386(1), pp.24-37.
- [9] Kolářová, L., Kučera, L., Vaňhara, P., Hampl, A. and Havel, J. (2015). Use of flower-like gold nanoparticles in time-of-flight mass spectrometry. *Rapid Communications in Mass Spectrometry*, 29(17), pp.1585-1595.
- [10] Lanni, E., Rubakhin, S. and Sweedler, J. (2012). Mass spectrometry imaging and profiling of single cells. *Journal of Proteomics*, 75(16), pp.5036-5051.
- [11] Guinan, T., Kirkbride, P., Pigou, P., Ronci, M., Kobus, H. and Voelcker, N. (2014). Surface-assisted laser desorption ionization mass spectrometry techniques for application in forensics. *Mass Spec Rev*, 34(6), pp.627-640.
- [12] Rainer, M., Qureshi, M. and Bonn, G. (2010). Matrix-free and material-enhanced laser desorption/ionization mass spectrometry for the analysis of low molecular weight compounds. *Anal Bioanal Chem*, 400(8), pp.2281-2288.
- [13] Le Pogam, P., Schinkovitz, A., Legouin, B., Le Lamer, A., Boustie, J. and Richomme, P. (2015). Matrix-Free UV-Laser Desorption Ionization Mass Spectrometry as a Versatile Approach for Accelerating Dereplication Studies on Lichens. *Analytical Chemistry*, 87(20), pp.10421-10428.
- [14] Chen, W., Tomalová, I., Preisler, J. and Chang, H. (2011). Analysis of Biomolecules through Surface-Assisted Laser, Desorption/Ionization Mass Spectrometry Employing Nanomaterials. *Jnl Chinese Chemical Soc*, 58(6), pp.769-778.
- [15] Kolářová, L., Vaňhara, P., Peňa Mendéz, E., Hampl, A. and Havel, J. (2014). Tissue visualization mediated by nanoparticles: from tissue staining to mass spectrometry tissue profiling and imaging. In: A. Seifalian, A. de Mel and D. M. Kalaskar, ed., *Nanomedicine*, 1st ed. Manchester: One Central Press (OCP), pp.467-488.
- [16] Tanaka, K., Waki, H., Ido, Y., Akita, S., Yoshida, Y., Yoshida, T. and Matsuo, T. (1988). Protein and polymer analyses up to m/z 100 000 by laser ionization time-of-flight mass spectrometry. *Rapid Communications in Mass Spectrometry*, 2(8), pp.151-153.
- [17] AQA, (2015). *Teaching notes: Time of flight mass spectrometry*. pp.1-9.
- [18] Sigma-Aldrich. (2016). *Custom DNA Oligos - QC Analysis by Mass Spectrometry*. [online] Available at: <http://www.sigmaaldrich.com/technical-documents/articles/biology/custom-dna-oligos-qc-analysis-by-mass-spectrometry.html> [Accessed 23 Apr. 2016].
- [19] Croxatto, A., Prod'hom, G. and Greub, G. (2012). Applications of MALDI-TOF mass spectrometry in clinical diagnostic microbiology. *FEMS Microbiology Reviews*, 36(2), pp.380-407.
- [20] Xiang, B. and Prado, M. (2010). An Accurate and Clean Calibration Method for MALDI-MS. *Journal of Biomolecular Techniques*, 21(3), pp.116-119.
- [21] Wolski, W., Lalowski, M., Jungblut, P. and Reinert, K. (2005). Calibration of mass spectrometric peptide mass fingerprint data without specific external or internal calibrants. *BMC bioinformatics*, 6:203
- [22] Webb, K., Bristow, T., Sargent, M. and Stein, B. (2004). *Methodology for accurate mass measurement of small molecules*. AccMass Best Practice Guide. Swansea: LGC Limited, pp.1-37.
- [23] Sládková, K., Houška, J. and Havel, J. (2009). Laser desorption ionization of red phosphorus clusters and their use for mass calibration in time-of-flight mass spectrometry. *Rapid Communications in Mass Spectrometry*, 23(19), pp.3114-3118.
- [24] Khan, AK., Rashid, R., Murtaza, G. and Zahra, A. (2014). Gold Nanoparticles: Synthesis and Applications in Drug Delivery. *Tropical Journal of Pharmaceutical Research*, 13(7), pp.1169-1177.
- [25] Kwon, K., Lee, K., Kim, M., Lee, Y., Heo, J., Ahn, S. and Han, S. (2006). High-yield synthesis of monodisperse polyhedral gold nanoparticles with controllable size and their surface-enhanced Raman scattering activity. *Chemical Physics Letters*, 432(1-3), pp.209-212.
- [26] Wang, W., Chen, Q., Jiang, C., Yang, D., Liu, X. and Xu, S. (2007). One-step synthesis of biocompatible gold nanoparticles using gallic acid in the presence of poly-(N-vinyl-2-pyrrolidone). *Colloids and Surfaces A: Physicochemical and Engineering Aspects*, 301(1-3), pp.73-79.
- [27] Xie, J., Zhang, Q., Lee, J. and Wang, D. (2008). The Synthesis of SERS-Active Gold Nanoflower Tags for In Vivo Applications. *ACS Nano*, 2(12), pp.2473-2480.
- [28] Yi, S., Sun, L., Lenaghan, S., Wang, Y., Chong, X., Zhang, Z. and Zhang, M. (2013). One-step synthesis of dendritic gold nanoflowers with high surface-enhanced Raman scattering (SERS) properties. *RSC Advances*, 3(26), p.10139.
- [29] Chemed.chem.purdue.edu. (2016). *The Chemistry of Nitrogen and Phosphorous*. [online] Available at: <http://chemed.chem.purdue.edu/genchem/topicreview/bp/ch10/group5.php> [Accessed 8 May 2016].
- [30] Shane, M. (2004). Tissue and cellular phosphorus storage during development of phosphorus toxicity in *Hakea prostrata* (Proteaceae). *Journal of Experimental Botany*, 55(399), pp.1033-1044.
- [31] Groves, R. and Keraitis, K. (1976). Survival and Growth of Seedlings of Three Sclerophyll Species at High Levels of Phosphorus and Nitrogen. *Australian Journal of Botany*, 24(6), p.681.

- [32] Ohnishi, M. and Razzaque, M. (2010). Dietary and genetic evidence for phosphate toxicity accelerating mammalian aging. *The FASEB Journal*, 24(9), pp.3562-3571.
- [33] Boone, M., Lin, Y., Meuris, L., Lemmens, I., Van Roy, N., Soete, A., Reumers, J., Moisse, M., Plaisance, S., Drmanac, R., Chen, J., Speleman, F., Lambrechts, D., Van de Peer, Y., Tavernier, J. and Callewaert, N. (2014). Genome dynamics of the human embryonic kidney 293 (HEK293) lineage in response to cell biology manipulations. *New Biotechnology*, 31, pp.S71-S72.
- [34] Cell lines service, (n.d.). *HEK 293*. CLS product information. Eppelheim: Cell lines service, pp.1-2.
- [35] Jiang, Y., Wu, X., Li, Q., Li, J. and Xu, D. (2011). Facile synthesis of gold nanoflowers with high surface-enhanced Raman scattering activity. *Nanotechnology*, 22(38), p.385601.
- [36] MERCK, (2015). *Triethanolamine*. Safety data sheet. Darmstadt: Merck KGaA, pp.1-9.
- [37] Shell chemicals, (2014). Ethylene Glycol. Safety data sheet. Singapore: Shell eastern trading (PTE) Ltd, pp.1-10.
- [38] Sigmaaldrich.com. (2016). *Gallic acid 97.5-102.5% (titration) | Sigma-Aldrich*. [online] Available at: <http://www.sigmaaldrich.com/catalog/product/sigma/g7384?lang=en®ion=CZ> [Accessed 20 May 2016].
- [39] Chen, T., Yu, C. and Tseng, W. (2014). Sinapinic acid-directed synthesis of gold nanoclusters and their application to quantitative matrix-assisted laser desorption/ionization mass spectrometry. *Nanoscale*, 6(3), pp.1347-1353.
- [40] Duan, J., Linman, M., Chen, C. and Cheng, Q. (2009). CHCA-modified Au nanoparticles for laser desorption ionization mass spectrometric analysis of peptides. *J Am Soc Mass Spectrom*, 20(8), pp.1530-1539.
- [41] Hajtmanová, K. (2015). *Mass spectrometry of retinoic acid*. Undergraduate. Masaryk University.
- [42] Connor, E., Mwamuka, J., Gole, A., Murphy, C. and Wyatt, M. (2005). Gold Nanoparticles Are Taken Up by Human Cells but Do Not Cause Acute Cytotoxicity. *Small*, 1(3), pp.325-327.
- [43] Shukla, R., Bansal, V., Chaudhary, M., Basu, A., Bhonde, R. and Sastry, M. (2005). Biocompatibility of Gold Nanoparticles and Their Endocytotic Fate Inside the Cellular Compartment: A Microscopic Overview. *Langmuir*, 21(23), pp.10644-10654.
- [44] Villiers, C., Freitas, H., Couderc, R., Villiers, M. and Marche, P. (2009). Analysis of the toxicity of gold nano particles on the immune system: effect on dendritic cell functions. *Journal of Nanoparticle Research*, 12(1), pp.55-60.
- [45] Noël, C., Simard, J. and Girard, D. (2016). Gold nanoparticles induce apoptosis, endoplasmic reticulum stress events and cleavage of cytoskeletal proteins in human neutrophils. *Toxicology in Vitro*, 31, pp.12-22.
- [46] Ramalingam, V., Revathidevi, S., Shanmuganayagam, T., Muthulakshmi, L. and Rajaram, R. (2016). Biogenic gold nanoparticles induce cell cycle arrest through oxidative stress and sensitize mitochondrial membranes in A549 lung cancer cells. *RSC Adv.*, 6(25), pp.20598-20608.
- [47] Mateo, D., Morales, P., Ávalos, A. and Haza, A. (2015). Comparative cytotoxicity evaluation of different size gold nanoparticles in human dermal fibroblasts. *Journal of Experimental Nanoscience*, 10(18), pp.1401-1417.
- [48] Sylvester, PW. Optimization of the Tetrazolium Dye (MTT) Colorimetric Assay for Cellular Growth and Viability. In: SD. Satyanarayanajois, ed., *Drug design and discovery*, 1st ed. Springer Science+Business Media, LLC, pp. 157-168.
- [49] Alkilany, A. and Murphy, C. (2010). Toxicity and cellular uptake of gold nanoparticles: what we have learned so far?. *Journal of Nanoparticle Research*, 12(7), pp.2313-2333.
- [50] Chithrani, B. and Chan, W. (2007). Elucidating the Mechanism of Cellular Uptake and Removal of Protein-Coated Gold Nanoparticles of Different Sizes and Shapes. *Nano Letters*, 7(6), pp.1542-1550.
- [51] Shen, Z., Sun, S., Wang, W., Liu, J., Liu, Z. and Yu, J. (2015). A black-red phosphorus heterostructure for efficient visible-light-driven photocatalysis. *J. Mater. Chem. A*, 3(7), pp.3285-3288.